Magnetic anisotropy parameters of matrix-isolated septet 1,3,5-trinitreno-2,4,6-trichlorobenzene

E. Ya. Misochko, A. V. Akimov, A. A. Mazitov, D. V. Korchagin, and S. V. Chapyshev*

Institute of Problems of Chemical Physics, Russian Academy of Sciences, 1 prosp. Akad. Semenova, 142432 Chernogolovka, Moscow Region, Russian Federation. E-mail: misochko@icp.ac.ru

An ESR spectrum of high-symmetry septet 1,3,5-trinitreno-2,4,6-trichlorobenzene generated under photolysis of 1,3,5-triazido-2,4,6-trichlorobenzene in solid argon at 15 K was recorded. Computer simulation revealed that the spectrum corresponds to the septet spin state with the fine structure parameters $D_S = -0.0957 \pm 0.0006$ cm^{-1} and $E_S = 0 \pm 0.0004$ cm^{-1}. These values of the magnetic anisotropy parameters D_S and E_S are in good agreement with the results of UDFT calculations. The spin-spin (D_{SS}) and spin-orbit (D_{SO}) coupling parameters of septet molecules with D_{3h} symmetry are negative and mutually enhance the magnetic anisotropy of these molecules. The contribution of the spin-orbit coupling to the magnetic anisotropy of 1,3,5-trinitreno-2,4,6-trichlorobenzene is higher than 11% due to the presence of three chlorine atoms in the molecule. This suggests the possibility of further strengthening the magnetic properties of septet 1,3,5-trinitrenobenzenes by introducing bromine and iodine atoms into positions 2, 4, and 6 of their benzene rings.

Key words: azides, nitrenes, photolysis, matrix isolation, ESR spectroscopy, high-spin states.

High-spin nitrene molecules represent ferromagnetic clusters bearing two or more unpaired electrons. Recently, high-spin nitrenes are used as model systems in studies of intramolecular magnetic interactions that play an important role in molecular magnetism, spintronics, and spin chemistry.[1—5] These interactions are responsible for the parameters of the fine structure tensor ($\hat{D}$) measured experimentally by ESR spectroscopy. As applied to the problems in question, investigations of high-spin molecules are of importance for progress in theoretical chemistry which needs high-precision experimental data for testing new quantum chemical methods of calculations in order to establish their predictive power in studies of complex magnetic systems. The first ESR spectra of high-spin organic molecules were recorded in the late 1960s.[6] Nevertheless, reliable methods of analysis of ESR spectra of powder samples with a complex pattern of ESR transitions between Zeeman energy levels under conditions where the parameters of zero-field splitting of the magnetic spin-Hamiltonian

$$\hat{H} = g\beta\mathbf{HS} + \mathbf{S}\hat{D}_S\mathbf{S} \qquad (1)$$

($\mathbf{H}$ is the magnetic field strength, $\hat{D}_S$ is the zero-field splitting tensor, $\mathbf{S}$ is the total spin, β is the electron Bohr magneton, and g is the electron g-factor) are comparable with the energy of RF-quanta were developed only in the last decade.[7—9] An analysis of ESR spectra using exact solutions to the magnetic spin-Hamiltonian (1) makes it possible to calculate the magnetic anisotropy parameter values with high accuracy.

Among organic hexaradicals, septet trinitrenes are characterized by the largest values of the magnetic anisotropy parameters $|D_S|$. According to theoretical estimates,[10] the energy of ferromagnetic exchange interaction between six unpaired electrons is ~3—10 kcal mol^{-1} which ensures a stable septet state ($S = 3$) even at room temperature. Recently, parameters of the $\hat{D}_S$ tensor were determined using the ESR spectra of some septet trinitrenes isolated in a solid argon matrix.[11—15] According to quantum chemical calculations,[3,4] the major contribution to the scalar parameters of the $\hat{D}_S$ tensor (D_S and E_S) comes from dipole-dipole spin-spin interactions between two unpaired electrons localized on the same nitrene center (so-called one-center interactions), whereas spin-spin interactions between unpaired electrons belonging to different nitrene atoms (two-center interactions) cause $|D_S|$ to decrease by about 30%. Parameters of the $\hat{D}_S$ tensor of septet trinitrenes are described with reasonable accuracy within the framework of the semiempirical model of three weakly interacting triplet centers[6,14—16]:

$$\hat{D}_S = (1/15)(\hat{D}_{T1} + \hat{D}_{T2} + \hat{D}_{T3}) + (1/15)\hat{D}_{ij}, \qquad (2)$$

where $\hat{D}_{Ti}$ are the tensors of the triplet nitrene centers and the $\hat{D}_{ij}$ tensor ($i, j = 1, 2, 3$) characterizes the interaction between the triplet centers.

Published in Russian in *Izvestiya Akademii Nauk. Seriya Khimicheskaya,* No. 12, pp. 2199—2205, December, 2012.

1066-5285/12/6112-2218

Molecules **1**—**4** with D_{3h} symmetry represent a particular type of septet trinitrenes. According to relation (2), in these molecules, the easy magnetization axis (Z axis of the $\hat{D}_S$ tensor) is directed normal to the molecular plane and the D_S parameter is negative, which is a key property of molecular magnets.[6,16] The E_S parameter of the $\hat{D}_S$ tensor characterizes the nonequivalence of the other two components; it is equal to zero because of high symmetry of the molecules.

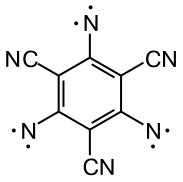

1

$D = -0.0548$
$E = 0$

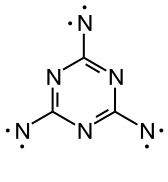

2

$D = -0.123$
$E = 0$

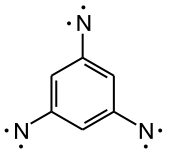

3

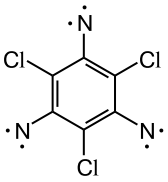

4

Note. From this point on, the D and E values are given in cm^{-1}.

Experimental data on the magnetic parameters of molecules **1**—**4** are scarce. An ESR spectrum of trinitrene **1** was reported;[6] however, the ESR spectrum *per se* was not presented and the $|D|$ parameter was estimated as 0.055 cm^{-1} using the resonance magnetic fields for three observed ESR lines and an approximate solutions to the spin-Hamiltonian (1). Then, a high-resolution ESR spectrum of septet trinitrene **2** isolated in solid nitrogen was described.[11] The $|D|$ parameter determined using this spectrum appeared to be equal to 0.123 cm^{-1}, being 2.2 times higher than that of trinitrene **1**. More recently,[14] an ESR spectrum of trinitrene **5** isolated in solid argon was recorded. Compound **5** can be treated as a close analog of a symmetric molecule of trinitrenobenzene **3**. The $|D|$ parameter of **5** is equal to 0.094 cm^{-1} and lies between those of trinitrenes **1** and **2**. Strongly different values of the magnetic anisotropy parameters of trinitrenes **1**, **2**, and **5** gave us an impetus to study paramagnetic products of photolysis of triazide **6** (Scheme 1) by matrix isolation ESR spectroscopy.

The most probable paramagnetic products of this photochemical reaction should include triplet nitrene **7**, quintet dinitrene **8**, and septet trinitrene **4**. Molecule **4** and trinitrene **1** have the same symmetry and substituents in their benzene rings are similar in electron-seeking properties. Therefore, the ESR spectra and magnetic parameters of trinitrenes **1** and **4** are expected to be similar. Our study was aimed to detect and analyze the ESR spectrum of trinitrene **4**, to determine the D_S and E_S parameters, to carry out a theoretical analysis of the main electronic interactions in the molecule, and to reveal factors governing the magnetic anisotropy in the septet aryltrinitrene molecules.

Scheme 1

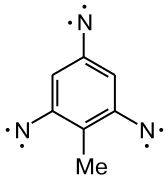

5

$D = -0.094$
$E = 0.004$

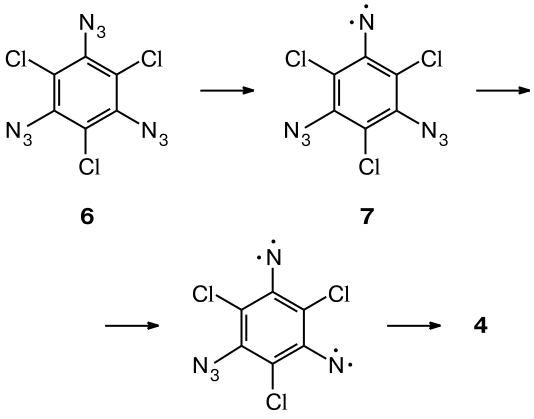

6 **7** **8** **4**

Experimental

IR spectrum was recorded with a Perkin—Elmer Spectrum 100 FT-IR instrument, UV spectrum was measured with a Specord M-80 spectrophotometer, and ^{13}C NMR spectrum was recorded with a Bruker Avance III spectrometer operating at 125 MHz. Mass spectrum was obtained on a Kratos MS-30 instrument with a direct inlet system (ionization energy 70 eV). Elemental analysis was performed on an Elementar Vario Microcube Elemental Analyzer CHNS/O. Commercially available 1,3,5-trifluoro-2,4,6-trichlorobenzene (Sigma—Aldrich) was used as is.

1,3,5-Triazido-2,4,6-trichlorobenzene (6). A solution of 1,3,5-trifluoro-2,4,6-trichlorobenzene (2.35 g, 10 mmol) and sodium azide (2.60 g, 40 mmol) in DMSO (20 mL) was stirred for 10 h at 60 °C and the reaction mixture was cooled to ~20 °C and poured in water (500 mL). The precipitate was filtered off, washed on the filter with water, dried in air, and recrystallized from EtOH. The yield was 2.92 g (96%), m.p. 93–94 °C.

IR spectrum (polycrystalline powder), ν/cm^{-1}: 2135, 2110 (N_3), 1528, 1411 (C=C, C=N), 1394, 1322 (N_3), 1254 (C—N), 1051, 955, 793, 728. Electronic absorption spectrum (EtOH), λ_{max}/nm (log ε): 202 (4.30), 250 (4.55), 272 (3.89). ^{13}C NMR spectrum ($CDCl_3$, δ): 121.3 (C—Cl), 134.8 (C—N_3). Mass spectrum, m/z (I_{rel} (%)): 305 $[M]^+$ (100). Found (%): C, 23.76; N, 41.29. $C_6Cl_3N_9$. Calculated (%): C, 23.67; N, 41.40.

Matrix isolation and ESR spectroscopy. The base unit of the experimental setup for cryogenic measurements and the procedure for ESR measurements were described in detail elsewhere.[7,12] Thin argon films were grown by vacuum co-condensation of two gas beams (argon and triazide **6**) on the substrate of a helium cryostat cooled to 15 K. The molecular beams were co-deposited on the lower end of a flat sapphire rod from two spatially separated nozzles. The diazide molecules were generated by sublimation of diazide powder placed in a quartz tube heated to ~87 °C with an external heater. The co-deposition regime was chosen preliminarily and provided an optimum deposition rate of molecules **6** in an Ar : **6** ≈ (10^3—10^4) : 1 ratio. The samples were at most 150 μm thick. After sample preparation the lower end of the sapphire rod was lowered to the center of the EPR spectrometer cavity. Photolysis at 15 K was carried out through a window in the cavity with light of a low-pressure mercury lamp (Mercury Spectral Line Lamp, Lot-Oriel) passed through an interference filter (Lot-Oriel, λ = 297 nm, FWHM ~5 nm).

ESR spectra were recorded with a Radiopan X-band spectrometer (Poland). A window in the cavity permitted on-site photolysis of the sample at 15 K. Impurity paramagnetic centers present in the sapphire rod show a number of narrow EPR lines. The EPR spectrum of the pure sapphire rod was recorded preliminarily; the corresponding lines are asterisked in the experimental spectrum (Fig. 1, *a*). The microwave power and modulation amplitude ensured no saturation effects in the ESR spectra recorded.

Computer simulation of ESR spectra was carried out using the *EasySpin* program package[17] based on the exact numerical diagonalization of the spin Hamiltonian (1).

Quantum chemical calculations. The geometry of molecules with the total spin $S = 3$ was optimized within the density functional theory (B3LYP/6-311G(d) approximation) using the Gaussian program.[18] The nature of stationary points was determined by analyzing the results of normal coordinate analysis (Hesse force constant matrix). Parameters of magnetic interactions including both spin-spin (SS) and spin-orbit (SO) coupling were obtained from single-point calculations based on the B3LYP/6-311G(d)-calculated geometries using the ORCA program package[19] with the PBE functional[20] and the Ahlrichs-DZ basis set.[21] The contributions of the SS- and SO-coupling to parameters of the $\hat{D}_S$ tensor were calculated by the McWeeny—Mizuno[22] and Pederson—Khanna[23] methods, respectively, implemented in the ORCA program package.[19] These methods provide good agreement between experimental data and calculated parameters of the $\hat{D}$ tensors for a number of high-spin nitrenes.[3] The $\hat{D}_S$ tensor was calculated by summation of the spin-spin and spin-orbit coupling tensors: $\hat{D}_S = \hat{D}_{SS} + \hat{D}_{SO}$. Sca-

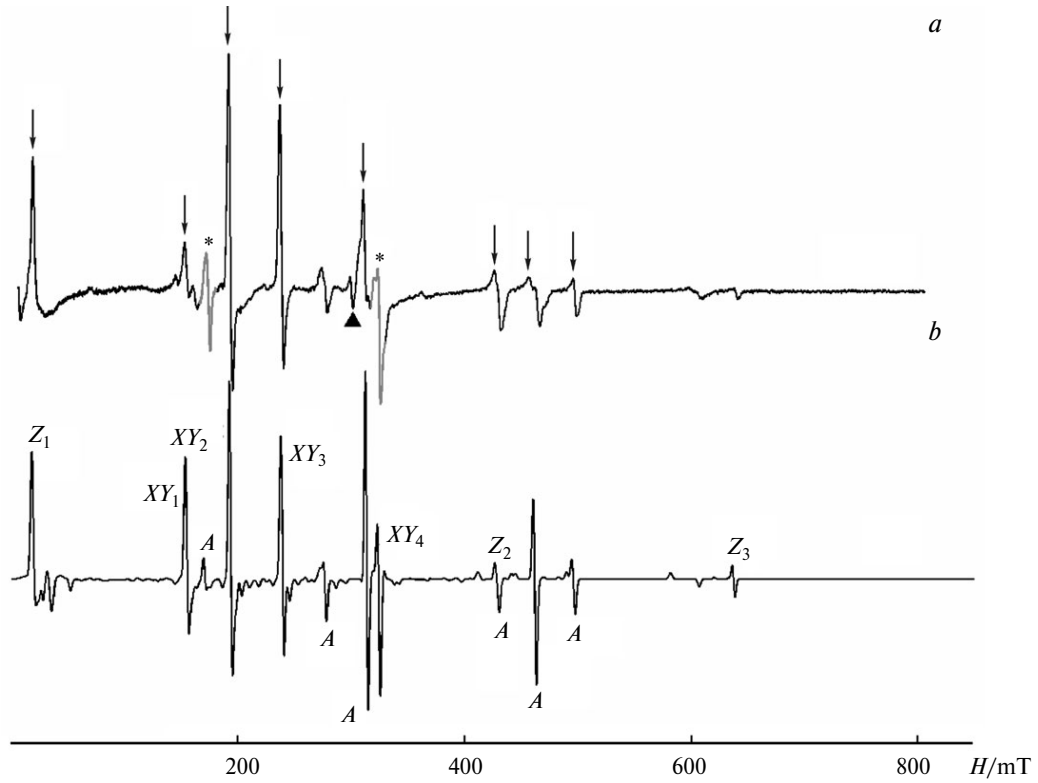

Fig. 1. (*a*) Experimental ESR spectrum of photolysis products of triazide **6** in argon matrix at 15 K; the signals of paramagnetic centers in the sapphire rod used as substrate are asterisked. (*b*) Theoretical ESR spectrum of the septet trinitrene with the magnetic anisotropy parameters $D_S = 0.0957\ cm^{-1}$ and $E_S = 0\ cm^{-1}$. Arrows show positions of the ESR lines in the experimental spectrum, which were used for optimization of the magnetic parameters of the trinitrene (see text). The microwave frequency is 9.107 GHz. Line assignment for the theoretical spectrum is given in accordance with Figs 2 and 3; here and in Figs 2 and 3, *A* denotes the extra lines.

lar parameters of the $\hat{D}_S$ tensor (D_S and E_S) were calculated conventionally:

$$D = (3/2)D_{zz},\ E = (D_{xx} - D_{yy})/2, \qquad (3)$$

where D_{xx}, D_{yy}, and D_{zz} are the eigenvalues of the $\hat{D}_S$ tensor.

Results and Discussion

Photolysis and ESR spectroscopy. ESR spectra of the unphotolyzed samples exhibit no lines from any paramagnetic species. Photolysis leads to the appearance of a series of lines with halfwidths ~1—2 mT in a wide range of magnetic field values. In the initial step of photolysis (~5 min), the ESR spectra exhibit lines appeared at resonance magnetic fields of 18, 153, 195, 238, 313, 429, 463, and 498 mT. Prolonged photolysis leads to an increase in the intensities of these lines and to the appearance of weak signals at 277, 300, 609, and 642 mT. Under long-term photolysis (>50 min), the line intensities reach maximum values and then slowly decrease. The ESR spectrum recorded at maximum line intensities is shown in Fig. 1, *a*. Earlier,[11—15] it was found that the ESR lines of triplet mononitrenes appear in the region 660—700 mT (x_2y_2 ESR transitions), which corresponds to $D_T \approx 0.95$—1.05 cm^{-1}. However, we failed to detect even weak lines of triplet mononitrene **7** in this range of magnetic field values. The ESR spectra of the quintet dinitrenes structurally similar to compound **8** are characterized by two strong lines (y_1 and y_2 ESR transitions) in the region 160 and 300 mT.[24—26] Typical ESR spectra of septet trinitrenes with $D_S \approx 0.1$ cm^{-1} exhibit a series of five or six strong lines in the region <400 mT; one or two of them appear in very low (less than 100 mT) magnetic fields.[11—15] These low-field ESR transitions are observed due to the fact that one zero-field splitting value equal to $|3D| \approx 0.3$ cm^{-1} is close to the energy of a microwave quantum of the X-band spectrometer.

The ESR spectrum shown in Fig. 1, *a* is similar to such spectra. Therefore, assuming that the eight strong spectral lines observed correspond to the septet trinitrene, we determined the parameters D_S and E_S of the magnetic interaction tensor by comparing the experimental spectrum with the theoretical spectra of a powder sample simulated based on exact solutions to the secular equation for the spin-Hamiltonian (1) for the system with the total spin $S = 3$. The starting parameters were $D_S = 0.1$ cm^{-1} and $E_S = 0$. To obtain the optimum theoretical spectrum, we minimized the R functional of the root-mean-square deviations of the experimental resonance magnetic fields from theoretical values by varying the D_S and E_S parameters:

$$R = \sqrt{\frac{1}{n}\sum_{k}^{n}[H_k(\text{calc}) - H_k(\text{exp})]^2}, \qquad (4)$$

where n is the number of spectral lines tested ($n = 8$). Positions of these lines are labeled in Fig. 1, *a*. The minimum value $R_{\min} = 0.73$ mT was obtained at $D_S = 0.0957$ cm^{-1}, $E_S = 0$, and $g = g_e = 2.0023$. This value is much smaller than the spectral line halfwidths and thus points to good agreement between theory and experiment. Both positions and relative intensities of resonance lines in the theoretical spectrum shown in Fig. 1, *b* agree well with those of the lines in the experimental spectrum. Also, the theoretical spectrum (see Fig. 1, *b*) shows that relatively weak lines at 277, 609, and 642 mT in the experimental spectrum also correspond to the septet trinitrene. Line assignment in the spectrum of septet trinitrene was based on the calculated transitions between Zeeman energy levels for the in-principal-axis orientations of the $\hat{D}_S$ tensor relative to the direction of external magnetic field. From Fig. 2 it follows that a number of strong spectral lines do not corre-

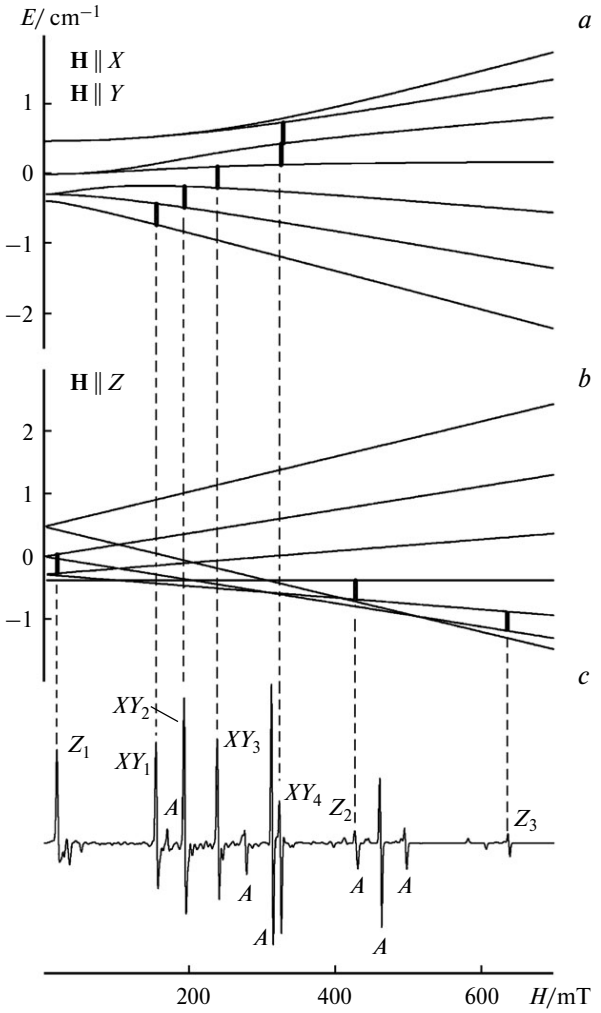

Fig. 2. Fine-structure energy levels (E) of the septet trinitrene with the parameters $D_S = 0.0957$ cm^{-1} and $E_S = 0$ cm^{-1} plotted *vs.* magnetic field for the in-principal-axis orientations of external magnetic field ($\mathbf{H} \parallel X$), ($\mathbf{H} \parallel Y$) (*a*), and ($\mathbf{H} \parallel Z$) (*b*). Vertical labels indicate the allowed ESR transitions; at $E_S = 0$ cm^{-1}, the X and Y principal axes of the $\hat{D}_S$ tensor are equivalent. (*c*) Theoretical ESR spectrum of powder sample.

spond to transitions in the in-principal-axis orientations. These lines are called extra lines. The theoretical plot of the angular dependence of resonance fields allows one to assign the extra lines. Analogous dependences for the transitions responsible for the extra spectral lines at resonance fields, where $(d\theta/dH) \to \infty$, are presented in Fig. 3.

The accuracy of determination of the D_S and E_S values was established using the plots shown in Fig. 4. These plots illustrate the increase in the R functional value when the D_S and E_S parameters are varied independently near their optimum values. The value $R_{cr} = 1.2$ mT at which the differences between the positions of lines in the experimental and theoretical spectra become larger than the linewidth was chosen as the critical value of the R functional. The errors in determination of the D_S and E_S parameters obtained using this procedure are ± 0.0006 and ± 0.0004 cm^{-1}, respectively.

A comparison of the experimental (see Fig. 1, *a*) and theoretical (see Fig. 1, *b*) spectra shows that only a weak line at 300 mT in the experimental spectrum does not correspond to the septet trinitrene. This line is labeled in spectrum 1, *a* by a triangle. Probably, this is a line of quintet dinitrene **8** because it is just the region near 300 mT where the strongest line in the ESR spectra of quintet dinitrenes are observed.[24—26] Note that photolysis of 1,3,5-triazido-2,4,6-tricyanobenzene and 2,4,6-triazido-1,3,5-triazine also results in the septet trinitrenes **1** and **2** as major products and that no ESR lines from intermediate dinitrenes were detected even in the early steps of photolysis. Contrary to this, studies on photolysis of some triazidopyridines[12,13,15] and 2,4,6-triazidotoluene[14] revealed successive formation of triplet mononitrenes, quintet dinitrenes, and septet trinitrenes.

Quantum chemical calculations of magnetic anisotropy parameters of septet trinitrenes. Table 1 lists the calculated values of the D_S parameters of trinitrenes **1**—**5**. For nitrenes **2**—**5**, the experimental and theoretical values are in good agreement. Systematic overestimation of $|D_S|$ by

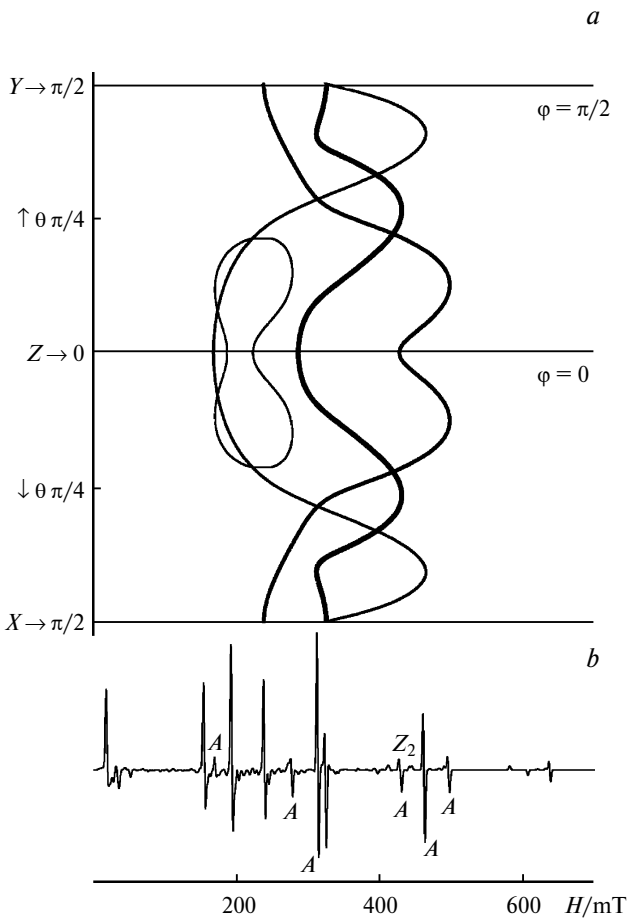

Fig. 3. (*a*) Positions of resonance magnetic fields plotted *vs.* angle θ at $\varphi = \pi/2$ (in the *zy* plane) and at $\varphi = 0$ (in the *zx* plane) for various transitions, where θ and φ are the Euler angles between the principal axes of the $\hat{D}_S$ tensor and the direction of external magnetic field. In the limiting cases ($\theta = 0$ and $\theta = \pi/2$) this corresponds to the in-principal-axis orientations of the $\hat{D}_S$ tensor. Calculations were carried out for the spectrum with the parameters $D_S = 0.0957$ cm^{-1} and $E_S = 0$. (*b*) The calculated ESR spectrum of powder sample.

Table 1. Theoretical and experimental values of magnetic anisotropy parameters (D/cm^{-1}) and the spin density values on the nitrene centers (ρ) in the septet trinitrenes **1**—**5**

Parameter[a]	**1**	**2**	**3**	**4**	**4Br**[b]	**5**
D_{exp}[c]	−0.055 [d]	−0.123 [e]	—	−0.096 [f]	—	−0.094 [g]
D_S (UDFT)	−0.103	−0.130	−0.109	−0.105	−0.242	−0.107
D_{SS} (UDFT)	−0.096	−0.121	−0.102	−0.093	−0.093	−0.100
D'_{SS} (UDFT)	−0.126	−0.152	−0.144	−0.139	—	−0.143
D_{SO} (UDFT)	−0.007	−0.009	−0.007	−0.012	−0.149	−0.007
ρ(N) (UDFT)	1.48	1.68	1.56	1.51	—	1.54, 1.56

[a] Calculated in the PBE/DZ approximation.
[b] Data taken from Ref. 27 (obtained from PBE/DZ calculations).
[c] The sign of the D_S parameter was not determined based on the ESR spectra. The "minus" sign was chosen in accordance with theory.
[d] Data taken from Ref. 6. [e] Data taken from Ref. 11. [f] This work. [g] Data taken from Ref. 14.

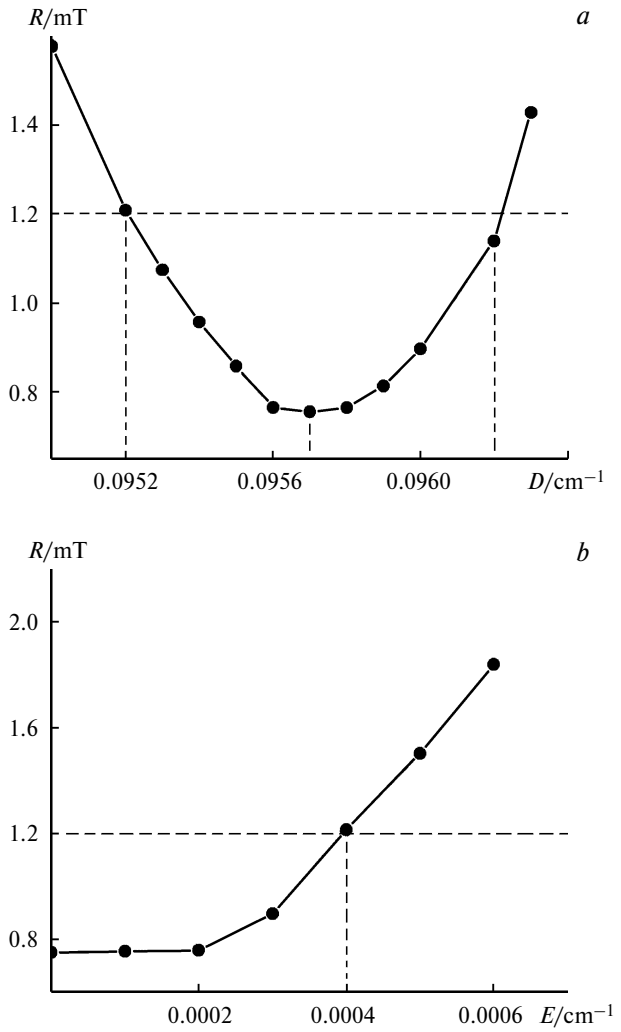

Fig. 4. The functionals, $R(D_S)$ (*a*) and $R(E_S)$ (*b*), of the root-mean-square deviations of the positions of eight lines in the calculated EPR spectrum from those in the experimental spectrum near the optimum values $D_S = 0.0957$ cm^{-1} and $E_S = 0$. The horizontal line shows the value of the functional R, which exceeds the linewidths in the experimental spectrum.

merely 6—10% obtained in calculations is typical of the computational method employed.[3] Note that among the tested molecules, the experimental value $|D_S| = 0.055$ cm^{-1} for trinitrene **1** seems strongly underestimated. According to calculations, the major contribution to the magnetic anisotropy comes from one-center spin-spin interactions in nitrene centers. The computational algorithm makes it possible to "extract" the energy of these interactions (D'_{SS}) from the total energy of spin-spin interactions D_{SS} (see Table 1). The highest degree of spin density localization on the nitrene centers ($\rho = 1.68$) is achieved for trinitrene **2** containing the smallest number of atoms in the molecule and three small nitrogen atoms in the aromatic ring. This trinitrene is characterized by the largest value of the magnetic anisotropy parameter $|D_S|$. As the number and size of atoms in the trinitrene molecules increases, $|D_S|$ decreases.

Figure 5 illustrates the character of spin density delocalization in trinitrene **4**. The spin density on the nitrene centers in molecule **4** is only slightly higher than that in trinitrene **1**. Therefore, both trinitrenes are characterized by very close theoretical $|D_S|$ values.

From the results of calculations it follows that none of the possible septet trinitrenes can compete with trinitrene **2** in magnitude of spin-spin interactions D_{SS}. The second component of the magnetic anisotropy coming from the spin-orbit coupling, D_{SO}, is very low for trinitrenes **1**—**3** and **5**. The principal axes of the $\hat{D}_{SS}$ and $\hat{D}_{SO}$ tensors coincide and both D_{SS} and D_{SO} values are negative. The contribution of the spin-orbit coupling to the total $|D_S|$ value is at most 7%. Trinitrene **4** containing chlorine atoms is characterized by the maximum $|D_{SO}|$ value for the septet molecules in question, which exceeds 11%. Even greater contribution of the spin-orbit coupling (~60%) to the total $|D_S|$ value was theoretically predicted for septet 1,3,5-tribromo-2,4,6-trinitrenobenzene (**4Br**).[27] Density functional calculations revealed a record-high value of the magnetic anisotropy parameter $|D_S|$ for trinitrene **4Br**, *viz.*, it is twice as large as that of trinitrene **2** (see Table 1).

Summing up, our analysis of experimental data obtained by ESR spectroscopy and the results of quantum chemical calculations suggests the following.

The magnetic anisotropy parameter D_S of septet trinitrenes **1**—**5** is determined by one-center spin-spin interactions between the unpaired electrons localized on the nitrene centers. The highest spin density on the nitrene centers and the strongest spin-spin interactions were found for the septet trinitrene molecule **2**. Compared to **2**, septet 1,3,5-trinitrenobenzenes bear a ~30% lower spin density on their nitrene centers and, correspondingly, are characterized by weaker spin-spin interactions. Molecule **4** contains three chlorine atoms and is characterized by an increase in the contribution of the spin-orbit coupling to the total magnetic anisotropy parameter $|D_S|$. The negative magnetic anisotropy of trinitrenobenzenes can be significantly increased by introducing bromine atoms into their

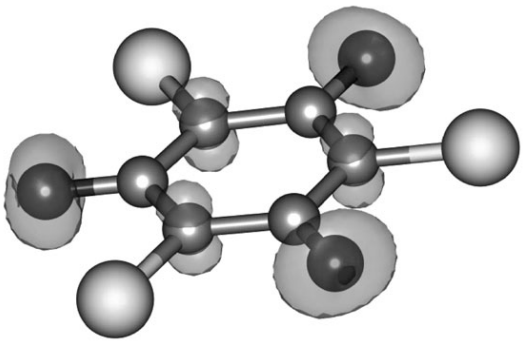

Fig. 5. Spin density distribution in the septet trinitrene **4** obtained from UDFT/PBE/DZ calculations.

molecules. This strategy of increasing the magnetic anisotropy of high-spin molecules seems to be more efficient compared to the attempts to synthesize high-spin molecules with the highest spin density on the triplet centers.

Trinitrene **4** studied in this work is characterized by close values of the spin density on the nitrene centers and the theoretical $|D_S|$ parameter with those of trinitrene **1**. It follows that the $|D_S|$ value reported previously for **1** is strongly underestimated and that the ESR spectrum of **1** should be very close to that of **4**. Our study confirmed that photolysis of 1,3,5-triazidobenzenes in cryogenic matrices results in septet trinitrenes as major products and that only trace amounts of intermediates (triplet mononitrenes and quintet dinitrenes) are formed, if any. High yield of septet trinitrenes in photolysis of 1,3,5-triazidobenzenes may appear to be of practical interest for obtaining magneto-active organic materials by low-temperature photolysis of crystalline triazides.

This work was financially supported by the Russian Foundation for Basic Research (Project No. 10-03-00065) and the Division of Chemistry and Materials Science of the Russian Academy of Sciences (Program No. 1).

References

1. F. Neese, *J. Chem. Phys.*, 2007, **127**, 164112.
2. W. Sander, D. Grote, S. Kossmann, F. Neese, *J. Am. Chem. Soc.*, 2008, **130**, 4396.
3. E. Ya. Misochko, D. V. Korchagin, K. V. Bozhenko, S. V. Chapyshev, S. M. Aldoshin, *J. Chem. Phys.*, 2010 **133**, 064101.
4. K. Sugisaki, K. Toyota, K. Sato, D. Shiomi, M. Kitagawa, T. Takui, *ChemPhysChem.*, 2010, **11**, 3146.
5. K. Sugisaki, K. Toyota, K. Sato, D. Shiomi, M. Kitagawa, T. Takui, *Phys. Chem. Chem. Phys.*, 2011, **13**, 6970.
6. E. Wasserman, K. Schueller, W. A. Yager, *Chem. Phys. Lett.*, 1968, **2**, 259.
7. E. Ya. Misochko, A. V. Akimov, V. F. Lavitskii, S. V. Chapyshev, *Russ. Chem. Bull.* (*Int. Ed.*), 2007, **56**, 2354 [*Izv. Akad. Nauk, Ser. Khim.*, 2007, 2284].
8. E. Ya. Misochko, A. V. Akimov, S. V. Chapyshev, *J. Chem. Phys.*, 2008, **128**, 124504.
9. T. Koto, K. Sugisaki, K. Sato, D. Shiomi, K. Toyota, K. Itoh, E. Wassermann, P. M. Lahti, T. Takui, *Appl. Magnet. Res.*, 2010, **37**, 703.
10. S. V. Chapyshev, R. Walton, J. A. Sanborn, P. M. Lahti, *J. Am. Chem. Soc.*, 2000, **122**, 1580.
11. T. Sato, A. Narazaki, Y. Kawaguchi, H. Niino, G. Bucher, D. Grote, J. J. Wolff, H. H. Wenk, W. Sander, *J. Am. Chem. Soc.*, 2004, **126**, 7846.
12. E. Ya. Misochko, A. V. Akimov, S. V. Chapyshev, *J. Chem. Phys.*, 2008, **129**, 174510.
13. S. V. Chapyshev, D. Grote, C. Finke, W. Sander, *J. Org. Chem.*, 2008, **73**, 7045.
14. S. V. Chapyshev, E. Ya. Misochko, A. V. Akimov, V. G. Dorokhov, P. Neuhaus, D. Grote, W. Sander, *J. Org. Chem.*, 2009, **74**, 7238.
15. S. V. Chapyshev, P. Neuhaus, D. Grote, W. Sander, *J. Phys. Org. Chem.*, 2010, **23**, 340.
16. K. Itoh, *Pure Appl. Chem.*,1978, **50**, 1251.
17. S. Stoll, A. Schweiger, *J. Magn. Reson.*, 2006, **178**, 42.
18. M. J. Fisch, G. W. Trucks, H. B. Schlegel, G. E. Scuseria, M. A. Robb, J. R. Cheeseman, J. A. Montgomery, Jr., T. Vreven, K. N. Kudin, J. C. Burant, J. M. Millam, S. S. Iyengar, J. Tomasi, V. Barone, B. Mennucci, M. Cossi, G. Scalmani, N. Rega, G. A. Petersson, H. Nakatsuji, M. Hada, M. Ehara, K. Toyota, R. Fukuda, J. Hasegawa, M. Ishida, T. Nakajima, Y. Honda, O. Kitao, H. Nakai, M. Klene, X. Li, J. E. Knox, H. P. Hratchian, J. B. Cross, V. Bakken, C. Adamo, J. Jaramillo, R. Gomperts, R. E. Stratmann, O. Yazyev, A. J. Austin, R. Cammi, C. Pomelli, J. Ochterski, P. Y. Ayala, K. Morokuma, G. A. Voth, P. Salvador, J. J. Dannenberg, V. G. Zakrzewski, S. Dapprich, A. D. Daniels, M. C. Stain, O. Farkas, D. K. Malick, A. D. Rabuck, K. Raghavachari, J. B. Foresman, J. V. Ortiz, Q. Cui, A. G. Baboul, S. Clifford, J. Cioslowski, B. B. Stefanov, G. Liu, A. Liashenko, P. Piskorz, I. Komaromi, R. L. Martin, D. J. Fox, T. Keith, M. A. Al-Laham, C. Y. Peng, A. Nanayakkara, M. Challacombe, P. M. W. Gill, B. Johnson, W. Chen, M. W. Wong, C. Gonazalez, J. A. Pople, *Gaussian 03. Revision D.01,* Gaussian Inc., Wallingford (CT), 2004.
19. F. Neese, *ORCA*, *An ab initio, Density Functional and Semiempirical Program Package*. *Version 2.8.0.2*, University of Bonn, Bonn, Germany, 2011; http://www.thch.uni-bonn.de/tc/orca.
20. J. P. Perdew, K. Burke, M. Ernzerhof, *Phys. Rev. Lett.*, 1996, **77**, 3865; J. P. Perdew, K. Burke, M. Ernzerhof, *Phys. Rev. Lett.*, 1997, **78**, 1396.
21. A. Schafer, H. Horn, R. Ahlrichs, *J. Chem. Phys.*, 1992, **97**, 2571; doi: 10.1063/1.463096.
22. R. McWeeny, Y. Mizuno, *Proc. R. Soc. London*, *Ser. A*, 1961, **259**, 554.
23. M. R. Pederson, S. N. Khanna, *Phys. Rev. B*, 1999, **60**, 9566.
24. T. A. Fukuzawa, K. Sato, A. R. Ichimura, T. Kinoshita, T. Takui, K. Itoh, P. M. Lahti, *Mol. Cryst. Liq. Cryst.*, 1996, **278**, 253.
25. S. V. Chapyshev, H. Tomioka, *Bull. Chem. Soc. Jpn*, 2003, **76**, 2075.
26. S. V. Chapyshev, *Izv. Akad. Nauk, Ser. Khim.*, 2006, 1085 [*Russ. Chem. Bull., Int. Ed.*, 2006, **55**, 1126].
27. E. Ya. Misochko, A. V. Akimov, A. A. Masitov, D. V. Korchagin, I. K. Yakushchenko, S. V. Chapyshev, *J. Chem. Phys.*, 2012, **137**, 064308.

Received August 22, 2012;
in revised form October 5, 2012